

EFFECT OF METAL ON THE PROPERTIES OF THE AZOPYRIDINE COMPLEXES OF IRON, RUTHENIUM AND OSMIUM

ABSTRACT

The theoretical study of α -, β -, γ -, δ -, ϵ - $MCl_2(Azpy)_2$ isomers with ($M = Fe, Os$ and Ru) complexes is carried out using **Density Functional Theory** (DFT) at the B3LYP / LANL2DZ level. This study is focused not only on the effect of metals over geometric, electronic and reactivity parameters, but also on their anti-cancer effect. Its results that the geometric parameters undergo small modifications. These modifications evolve from iron to osmium through ruthenium complexes. Thus, the lengths of the bonds $M-X$ (with $X = Cl, N_2, N_{py}$) follow the following order $Fe-X < Ru-X < Os-X$. However, regarding their angular variation that undergoes deformation through the octahedron shape, it could be related to **Jahn** Teller effect. Also, the substitution of Ru by Os would increase the reactivity of these complexes. Among the isomers studied, the ϵ - Fe , δ - Ru and δ - Os complexes are likely to bind easily to the DNA. The values of the dipole moments are arranged in the following order: $\mu(\epsilon-M) > \mu(\beta-M) > \mu(\alpha-M) > \mu(\gamma-M) > \mu(\delta-M)$ within these azopyridine complexes. **Finally, we notice that the substitution of Ru by Os improves the cytotoxicity and the fluorescence of these complexes.** The δ - Os isomer has the best cytotoxic and photosensitive characteristics of these azopyridine complexes and would be the ideal isomer for the diagnosis and treatment of cancers.

Keywords: Cancer, azopyridine, fluorescence, DFT, TDDFT, iron, ruthenium, osmium.

1. INTRODUCTION

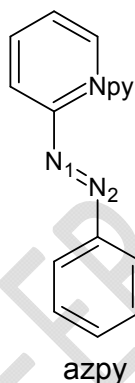
The cancer remains today one of the most dangerous diseases to be eradicated despite the improvement in its detection, its prevention and its treatment. Some cancers can be caused by smoking, obesity, physical inactivity and infections [1]. Several treatment methods such as chemotherapy exist, yet they have many failures that can sometimes be related to metastases and side effects. Therefore, current research focuses on methods or drugs that combine efficacy and low side effects. Since the successful development of $cis-[PtCl_2(NH_3)_2]$ (cisplatin) [2] as a cancer drug, many efforts are based on the development of transition metal-based drugs thanks to their high clinical efficacy, the reduction of systemic toxicity and the prolonged multiple activity in which cisplatin is even totally inactive. The low oxidation states $Ru(II)$ or $Ru(III)$ compounds are considered suitable candidates for the implementation of anticancer drugs, since the kinetics of the substitution reactions of their ligands is like those of platinum (II) compounds. Some of these drugs have been shown to be highly effective against metastases of solid tumors in both experimental tumors and human tumors grafted in nude mice [3, 4]. Since then, azopyridine $Ru(II)$ complex is the subject of intense research.

Azopyridines ligands are organic compounds consisting of a pyridine group and an aromatic ring, linked together by an azo bond $N=N$. The electron-rich azo group ($-N=N-$) gives some rigidity to the azopyridine ligand. The arylazopyridine complexes of $Ru(II)$, $Ru(Azpy)_2Cl_2$ where $Azpy$ stands for 2-phenylazopyridine, represent a class of well-characterized anticancer compounds. There are five well known different isomers of these complexes owing to the unsymmetry of the ligand [5]. Their activity has a strong structural dependence [6]. Reedijk et al. reported that the elevated cytotoxicity of α and γ isomers in vitro (A498, EVSA-T, H226, IGROV, MCF-7, WIDR, M19 cells) were compared to cisplatin and 5-fluorouracil, which are approximately 10 times higher than the corresponding β isomer [7]. Modifications have been made to these isomers to improve their cytotoxic characteristics. However, the addition of methyl groups to the pyridine or phenyl ring, giving respectively $Ru(tazpy)_2Cl_2$ and $Ru(mazpy)_2Cl_2$ ($tazpy = o$ -tolylazopyridine and $mazpy = 4$ -methyl-2-

49 phenylazopyridine) did not alter the rank of cytotoxicity given by the SAR (structure-activity
50 relationship) study over the starting isomers. Other modifications have been undertaken to
51 improve the solubility of these azopyridine complexes. For instance, water-soluble
52 derivatives of the α -isoform where the chloride ligands are replaced by nitrate, 1,1-
53 cyclobutanedicarboxylate, oxalate or malonate ligands have been developed but all these
54 complexes were found less cytotoxic than the α isomer (A2780, A2780cisR). Nevertheless,
55 their activity remains comparable to carboplatin's [8]. The structural characteristics of these
56 compounds have a significant impact on the effectiveness of cytotoxic compounds.

57 In a recent work, we studied the effect of halogen atoms on the activity of $\text{RuX}_2(\text{Azpy})_2$ where X stands
58 for F, Cl, Br and I. we showed that the strength of activity of the complex evolves according to
59 electronegativity of halide atoms. Thus, complexes $\text{RuF}_2(\text{Azpy})_2$ were discovered to be the most active
60 molecules [9].

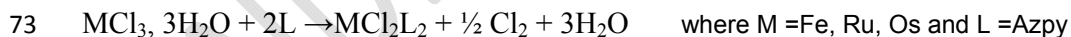
61 Here, we want to evaluate by means of theoretical tools, the effect of certain metals on the anti-cancer
62 properties of azopyridine complexes. The metals chosen are Fe, Ru and Os. Their common
63 particularity is that they belong to the same group of the periodic table. Hence, they must form the
64 same number of isomers. Moreover, the ligand chosen for the complexation of these metals remains
65 the well-studied 2-phenylazopyridine which structure is displayed in Figure 1.

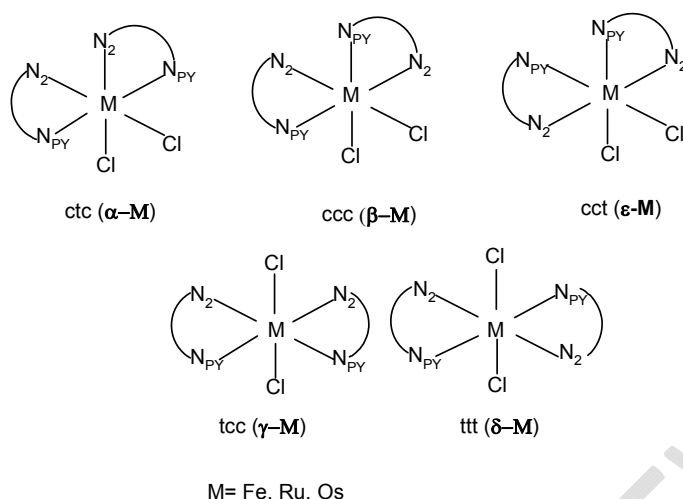


66

67 Figure 1: Ligand Azpy with three nitrogen atoms and the ligand is assumed to bind the metal by both
68 N_2 and N_{py} as to highlight its bidentate state. This ligand is used to form a ring of five atoms with the
69 metal.

70 According to previous papers, we showed that five complexes are always formed between Azpy ligand
71 and any metal atom as illustrated in the Figure 2 [5]. These isomers are formed according to the
72 following reaction:





74

75 Figure 2. The five isomers likely to form with the azopyridine ligand. All these isomers are of C_2
 76 symmetry except the β isomer. Here, α -M, β -M and ϵ -M are the cis complexes while γ -M and δ -M
 77 represent both the trans isomers.

78

79 2. METHOD OF CALCULATIONS

80 2.1. DFT Calculations

81 The optimization of the molecules was carried out in the gas phase using GAUSSIAN 09 software
 82 [10]. The minimal energy structure was performed using density functional theory (DFT). All DFT
 83 calculations were performed using the Becke B3LYP 3-parameter hybrid functional [11, 12, 13, 14]
 84 and the basis set containing the double zeta pseudo-potential Lanl2DZ [15, 16]. Today, the DFT
 85 method allows to clarify many chemical phenomena in a wide variety of fields that encompasses
 86 energy production (photovoltaic, fuel cells, nuclear), geochemistry (minerals, the earth's core) and
 87 biology (enzymes, proteins, DNA). In the latter field for example, the study of enzymatic catalysis, has
 88 allowed the rationalization of experimental data and the elucidation of reaction mechanisms for many
 89 enzymes [16]. The geometry optimizations were performed at fundamental states of these complexes
 90 and they were assumed to be in a singlet state [17]. In addition, the stable configuration of the
 91 isomers was confirmed by frequency analysis in which no imaginary data was observed for all
 92 minimum energy configurations. Therefore, DFT methods with B3LYP and Lanl2dz basis set are
 93 assumed so far to be consistent with experiment data performed on ruthenium complexes [13]. The
 94 energy of Frontier molecular orbitals (HOMO and LUMO) were analyzed. The analysis of the natural
 95 orbital population NPA was also carried out.

96

2.2. Spectral Constant

97 The excitation of a molecule or an atom without an external magnetic field during an average
 98 time $\tau = 1,499/f.E^2$ can allow a photo emission [18]. Here f represents the oscillation
 99 force of the transition and E the wavenumber of excitation expressed in cm^{-1} . τ represents
 100 the life time of the excited state. Besides, the coefficients probability of Einstein's transition
 101 given by A_{if} for emission and B_{if} for absorption between the initial (i) and final (f) electronic
 102 states are given as follows [19] :

$$103 A_{if} = 1 / \tau$$

104 where τ is the life time expressed in seconds.

105 $B_{if} = 14,50 \cdot 10^{24} D_{if}$

106 where D_{ij} is the dipole moment of transition. In general, the dipole moment of transition can
 107 be obtained by the following relation:

108 $D_{ij} = 4,24 \cdot 10^{-20} \cdot \frac{c\hbar}{\nu} \varepsilon_{max}$, where \hbar is the half-width of the absorption band in cm^{-1} , ε_{max} the
 109 molar extinction coefficient and c the speed of light, $3 \times 10^{10} \text{ cm s}^{-1}$, ν the radiation frequency
 110 in s. Specific indices of reactivity [20, 21] have been established according to the following
 111 relationships:

- 112 ➤ chemical potential $\mu = (\varepsilon(HOMO) + \varepsilon(LUMO)) / 2$,
- 113 ➤ the absolute chemical hardness $\eta = (\varepsilon(LUMO) - \varepsilon(HOMO)) / 2$,
- 114 ➤ electrophilia $\omega = \mu^2 / 2\eta$,
- 115 ➤ nucleophilia $N = \varepsilon HOMO(Nu) - \varepsilon HOMO(TCE)$, where tetracyanoethylene (TCE)
 116 is the reference because it has the lowest energy of the HOMO among the series of
 117 molecules already explored in the context of organic polar reactions [19].

118 3. RESULTS AND DISCUSSION

119 3.1 The geometrical parameters

120 The geometrical parameters regard the metallic bonds that are assumed to influence the shape of the
 121 molecules. Those bonds are M-Cl, M-N₂ and M-N_{py}. Both chloride atoms have sometime different
 122 bonding to the metal. So, they are numbered to emphasize the difference between both bondings that
 123 can be at the origin of a symmetry. Besides, the distance between the two nitrogen atoms within the
 124 ligand forming the azo group (N=N) which confers a certain rigidity to the ligand can also undergo a
 125 modification. Moreover, several angles formed with the metal like Cl₁-M-Cl₂, N_{py}-M-N_{py} and N₂-M-N₂
 126 vary from a molecule to another. Table 1 display these geometrical parameters.

127 Table 1 : Geometric parameters of Azpy complexes at B3LYP / LANLD2Z level; lengths are set in (Å)
 128 and angles are in (°).

		N ₁ =N ₂	M-N ₂	M-N _{py}	M-Cl ₁	M-Cl ₂	Cl ₁ -M-Cl ₂	N _{py} -M-N _{py}	N ₂ -M-N ₂
α -Fe	Calc	1.31	1.94	1.96	2.39	2.39	92.58	177.76	100.31
β -Fe	Calc	1.31-1.31	1.98-1.95	1.96-1.97	2.39	2.39	93.59	96.23	104.16
γ -Fe	Calc	1.30	1.99	1.98	2.39	2.39	176.12	103.87	98.18
δ -Fe	Calc	1.30	1.98	2.01	2.40	2.40	180.00	166.73	171.24
ε -Fe	Calc	1.31	1.96	1.97	2.39	2.39	96.98	90.25	172.35
α -Ru	Calc	1.32	2.03	2.06	2.48	2.48	90.58	178.37	101.51
	Exp	1.28	2.03	2.05	2.40	2.40	89.50	174.50	93.50
β -Ru	Calc	1.32-1.32	2.02-2.05	2.05-2.07	2.48	2.48	90.18	99.21	104.58
	Exp	1.29-1.30	1.96-2.00	2.02-2.06	2.40	2.41	91.10	101.90	103.00
γ -Ru	Calc	1.32	2.03	2.10	2.48	2.48	170.71	102.86	104.99
	Exp	1.31	1.99	2.11	2.38	2.38	170.50	103.80	104.10
δ -Ru	Calc	1.31	2.06	2.10	2.49	2.51	180.00	167.53	178.58
	Exp	1.28	2.02	2.06	2.38	2.38	180.00	180.00	180.00
ε -Ru	Calc	1.32	2.05	2.06	2.49	2.49	94.10	93.58	169.48
α -Os	Calc	1.34	2.00	2.05	2.48	2.48	88.36	178.92	101.43
β -Os	Calc	1.34-1.34	2.02-1.99	2.07-2.04	2.47	2.48	87.84	99.64	103.56
γ -Os	Calc	1.34	2.00	2.10	2.47	2.47	166.67	103.95	104.49
δ -Os	Calc	1.32	2.03	2.08	2.50	2.50	180.00	169.42	175.25
ε -Os	Calc	1.34	2.03	2.05	2.48	2.48	91.24	168.64	96.17

130 In general, the bond's lengths undergo a variation which depends on the nature of the metal
131 atom. Since all metal belong to the same group in the periodic table, the lengths M-X with M
132 = Fe, Ru, Os and X = Cl, N₂, N_{Py} such as M-Cl, M-N₂ and M-N_{Py} follow the same trends
133 depending on the metallic shape. Indeed, the lengths MX increase from Fe to Os atoms.
134 Therefore, we have the following classifications: Fe-Cl < Ru-Cl < Os-Cl; Fe-N₂ < Ru-N₂ < Os-N₂
135 and Fe-N_{Py} < Ru-N_{Py} < Os-N_{Py}. Likewise, the bonding of the azo group follows the same
136 order with Fe (N=N) < Ru (N=N) < Os (N=N). From this analysis, we can conclude that the
137 metallic substitution triggers an elongation of the distance between the metal atom and the
138 atoms directly linked to it. This elongation within these complexes is certainly due to the
139 electronegativity of metal atoms [22]. According to the Pauling scale, the electronegativities
140 of these metal atoms are 1.83 and 2.2 respectively for iron and for both ruthenium and
141 osmium. Here, the identical electronegativity of both Ru and Os atoms explains the
142 proximity of their bondings in the complexes. Moreover, it is found that the values obtained
143 theoretically and experimentally regarding Ru isomers are in good agreement. Furthermore,
144 we notice that the metal has no influence on the deformation of the octahedral structure of
145 these complexes insofar that the Cl₁-M-Cl₂ angle remains the same for all the δ-M isomers.
146 The particularity of this isomer is that both Cl atoms are different. Also, it has a C₂ axis of
147 symmetry that passes through the two chlorine and the metal atoms. Therefore, we assume
148 that this configuration reduces Coulomb repulsions due to the high electronegativity of the
149 chlorine atoms which is 3.16 according to the Pauling scale. Regarding the other isomers
150 such as α-M, γ-M and ε-M, they also have a C₂ axis of symmetry, but this axis does not pass
151 through the two chlorine atoms and the metal atom. Moreover, they have all their atoms
152 identical by pair thereby justifying their C₂ symmetry. Whereas the β-M isomer, it has no C₂
153 axis of symmetry and all atoms are different. Yet, all five isomers display a deformation of the
154 octahedron. Therefore, the octahedral deformation of these complexes must certainly be
155 caused by Jahn Teller effect [23] through which frontier orbitals degenerate for the
156 complexes' stabilizations. it results from that analysis that whatever the nature of the metal,
157 Azpy ligand imposes the structure of the complex.

158 3.2 Electronic Structure Parameters and reactivity

159 3.2.1. Free Enthalpy and Frontier Molecular Orbital Analysis

160 Table 2 displays the frontier molecular orbitals HOMO (the highest occupied molecular orbital) and
161 LUMO (lowest unoccupied molecular orbital), the energetic gap and the free enthalpy of reaction.
162 These parameters are specifically known to indicate the global reactivity of molecules. Besides,
163 HOMO and LUMO orbitals are determining parameters in the field of quantum chemistry [24]. They
164 define the electron density at the boundaries for the prediction of the most reactive positions in π
165 electron systems. They determine the ability of the molecule to interact with other molecules. The
166 HOMO energy determines the molecule's ability to donate electrons while the LUMO energy evaluates
167 the ability for the molecule to accept electrons [25, 26, 27, 28]. The gap energy is also used to
168 characterize the chemical reactivity and the kinetic stability of the molecule. A molecule with a weak
169 gap is more polarizable and generally it is associated with a high chemical reactivity including a low
170 kinetic stability and it is also called a soft molecule [5]. Molecules possessing a conjugation system are
171 characterized by a low value of the electronic gap energy. The gap also reflects the level of charge
172 transfer between the electron-donor group and the electron-acceptor group via the conjugation within
173 the molecule. The thermodynamic values ΔG° describes the stability of these azopyridine complexes.

174

175

176

177 Table 2: Global reactivity parameters: frontier molecular orbitals HOMO and LUMO, energy gap and
 178 free enthalpy reaction in Kcal.mol⁻¹ at B3LYP/LANLD2Z level.

Isomers	E_{HOMO}	E_{LUMO}	$\Delta E_{\text{L-H}}$	ΔG°
α -Fe	-5,633	-3,276	2,357	6,360
β -Fe	-5,523	-3,276	2,247	10,330
γ -Fe	-5,648	-3,279	2,369	14,470
δ -Fe	-5,588	-3,277	2,311	11,680
ϵ -Fe	-5,554	-3,352	2,202	11,110
α -Ru	-5,553	-3,332	2,221	-16,520
β -Ru	-5,525	-3,224	2,301	-13,330
γ -Ru	-5,385	-3,366	2,019	-8,530
δ -Ru	-5,229	-3,431	1,798	-9,640
ϵ -Ru	-5,403	-3,362	2,041	-10,410
α -Os	-5,572	-3,306	2,266	-38,090
β -Os	-5,547	-3,151	2,396	-34,930
γ -Os	-5,335	-3,350	1,985	-27,780
δ -Os	-5,074	-3,426	1,648	-24,800
ϵ -Os	-5,395	-3,255	2,140	-30,240

179

180 Through ΔG° , we can assume that the synthesis of these complexes is spontaneous at room
 181 temperature under 1 atmosphere except for Fe where the synthesis requires an energy to be provided
 182 for all its isomers owing to the positive values of ΔG° . Moreover, Os complexes are assumed to be the
 183 most stable due to their lowest values of ΔG° . In the same trend, the least stable complexes are Fe
 184 complexes with the highest values of ΔG° . Therefore, it results from this analysis regarding the
 185 stability that it increases downwardly from Fe to Os in respect of the periodic table. Hence, the stability
 186 of the complex increases with the shape of the metal. Moreover, we can notice particularly that the
 187 most stable complex regarding each metallic atom is α -M isomer.

188 Regarding the gap energy, Table 2 shows that the most chemically stable isomers are ϵ -Fe, δ -Ru and
 189 δ -Os. These isomers are noticed to be also the most polar and the most kinetically stable. Besides, δ -
 190 Os is assumed to be the most candidate as photosensitizer. Furthermore, the electronic interaction of
 191 these complexes with other molecules can be two forms: either these complexes will act as
 192 nucleophiles, or they will act as electrophiles. In the case of a nucleophilic reaction, the reactivity of
 193 these complexes will be evaluated from the HOMO energies of these complexes and the most active
 194 will be that will have the highest HOMO energy. In the case of an electrophilic reaction, the reactivities
 195 of these complexes will be evaluated from the LUMOs of these complexes and the most active will be
 196 that having the lowest LUMO energy. In general, the reactivity of these complexes increases
 197 downward in the period. In order to evaluate the activities of these complexes, we have established
 198 their order of magnitude in Table 3.

199

200 Table 3: Order of magnitude of the energies of the HOMO and LUMO orbitals of the Azpy complexes

Frontier Orbitals	Order of energy
HOMO	$E_{\text{HOMO}}(\gamma\text{-Fe}) < E_{\text{HOMO}}(\alpha\text{-Fe}) < E_{\text{HOMO}}(\delta\text{-Fe}) < E_{\text{HOMO}}(\varepsilon\text{-Fe}) < E_{\text{HOMO}}(\beta\text{-Fe})$
	$E_{\text{HOMO}}(\alpha\text{-Ru}) < E_{\text{HOMO}}(\beta\text{-Ru}) < E_{\text{HOMO}}(\varepsilon\text{-Ru}) < E_{\text{HOMO}}(\gamma\text{-Ru}) < E_{\text{HOMO}}(\delta\text{-Ru})$
	$E_{\text{HOMO}}(\alpha\text{-Os}) < E_{\text{HOMO}}(\beta\text{-Os}) < E_{\text{HOMO}}(\varepsilon\text{-Os}) < E_{\text{HOMO}}(\gamma\text{-Os}) < E_{\text{HOMO}}(\delta\text{-Os})$
LUMO	$E_{\text{LUMO}}(\varepsilon\text{-Fe}) < E_{\text{LUMO}}(\gamma\text{-Fe}) < E_{\text{LUMO}}(\delta\text{-Fe}) < E_{\text{LUMO}}(\alpha\text{-Fe}) < E_{\text{LUMO}}(\beta\text{-Fe})$
	$E_{\text{LUMO}}(\delta\text{-Ru}) < E_{\text{LUMO}}(\gamma\text{-Ru}) < E_{\text{LUMO}}(\varepsilon\text{-Ru}) < E_{\text{LUMO}}(\alpha\text{-Ru}) < E_{\text{LUMO}}(\beta\text{-Ru})$
	$E_{\text{LUMO}}(\delta\text{-Os}) < E_{\text{LUMO}}(\gamma\text{-Os}) < E_{\text{LUMO}}(\alpha\text{-Os}) < E_{\text{LUMO}}(\varepsilon\text{-Os}) < E_{\text{LUMO}}(\beta\text{-Os})$

201

202 Table 3 indicates that for a nucleophilic reaction of these complexes, the most active
 203 complexes are β -Fe, δ -Ru and δ -Os isomers. However, regarding the electrophilic reactions, the most
 204 active complexes are ε -Fe, δ -Ru and δ -Os isomers. For Ru and Os complexes anyway, we can see
 205 that δ -M represent both the nucleophile and the electrophile confirming the gap energy classification.
 206 However, concerning Fe, there is no real stability. From this analysis, we can say that the metallic
 207 substitution within the azopyridine complexes modifies their reactivity. Besides, the substitution of Ru
 208 by Os increases the reactivity of these complexes.

209 3.2.2. Dipole Moment

210 The measurement of the ability of a molecule in chemistry to interact with the water molecules through
 211 hydrophilicity is determined by the log P value. In fact, the value of Log P expresses the solubility of
 212 the compound in an organic solvent or in water. The hydrophilic notion can be evaluated by the dipole
 213 moment. In fact, the dipole moment indicates the solubility force in water of a molecule. Accordingly, a
 214 high value of this dipole moment implies only low solubility in an organic solvent and high solubility in
 215 water. In fact, the most effective drugs are fat-soluble because many anti-metastatic drugs work in
 216 organic solvents [5]. Thus, the table presents the dipole moments of the isomers of Fe, Ru and Os
 217 azopyridine complexes.

218 Table 4: Dipolar momentum of the azopyridine complexes.

Isomers	Dipole Moment			
	x	y	z	Total
α - Fe	0,00	0,00	-7,42	7,42
β - Fe	-2,80	1,77	8,61	9,22
γ - Fe	0,00	0,00	1,92	1,92
δ - Fe	0,00	0,00	1,28	1,28
ε - Fe	0,00	0,00	-10,04	10,04
α - Ru	0,00	0,00	-7,26	7,26
β - Ru	-1,74	0,97	8,60	8,83
γ - Ru	0,00	0,00	1,68	1,68
δ - Ru	0,00	0,00	-1,33	1,33
ε - Ru	0,00	0,00	-10,02	10,02
α - Os	0,00	0,00	-6,53	6,53
β - Os	-1,48	0,59	7,94	8,10
γ - Os	0,00	0,00	1,78	1,78
δ - Os	0,00	0,00	-0,79	0,79
ε - Os	0,00	0,00	-9,09	9,09

219

220 Table 4 contains the dipole moments of the isomers of each metal complex. We can notice that the
 221 values of these dipole moments are arranged for each group of isomers in the following order: μ (ϵ -
 222 M) $>$ μ (β -M) $>$ μ (α -M) $>$ μ (γ -M) $>$ μ (δ -M) within the azopyridine complex. Hence, we can retain that the
 223 order of solubility of these isomers does not depend on the nature of the metal atom, but it depends on
 224 all the structure. Therefore, the most soluble isomers in organic solvents are those where both **chloride**
 225 **atoms** are in *trans* position. However, when it comes to compare each isomer of the three metals, the
 226 solubility increases as usual from Fe to Os and specifically, the most soluble is assumed to be the δ -
 227 Os isomer. Whereas for the aqueous solvents, the ϵ -Cl isomers present the greatest values regarding
 228 their solubility therein. This solubility also decreases from Fe to Os. Furthermore, the isomers having
 229 the chlorine atoms in the *trans* position (γ -M and δ -M) are more active in organic medium than those
 230 which have the chlorine atoms in the *cis* position (α -M, β -M and ϵ -M). Thus, it results that osmium
 231 increases the cytotoxicity of the complex irrespective of the isomer.

232 3.2.3. Atomic Net Charge

233 To study the metal-ligand interactions in all isomers of the $\text{FeCl}_2(\text{Azpy})_2$, $\text{RuCl}_2(\text{Azpy})_2$ and
 234 $\text{OsCl}_2(\text{Azpy})_2$ complexes, we used the NBO analysis method. This analysis was performed
 235 on the gas phase optimized structures of the isomers at B3LYP/LanI2DZ level. Calculation of
 236 the natural charges on both the metal atom and the ligands made it possible to understand
 237 the global charge transfer from ligands to the metal and vice versa and the contributions of
 238 each ligand to this charge transfer. Moreover, the calculation of NBOs, the analysis Donor-
 239 acceptor interactions between the NBOs of the metals and ligands made it possible to
 240 evaluate the relative σ -donor and π -acceptor character of each ligand in all the isomers of
 241 the complexes. It is important to recall that the optimized geometries of the α -M, γ -M, δ -M
 242 and ϵ -M isomers have a C_2 symmetry which makes the charges carried by both Azpy ligands
 243 on the one hand and by both chlorine atoms on the other hand identical. The natural charges
 244 carried by the metal atoms (Fe, Ru and Os) and each ligand in all the isomers of the
 245 complexes at the ground state are given in Table 5.

246 Table 5: Natural Charges of the Metal atoms (M = Fe, Ru and Os), Cl atoms and Azopyridine ligands
 247 of Complexes at B3LYP/LanID2Z Level.

Isomers	Total Natural charge		
	M	Ligand	Cl
α -Fe	-0.02	0.84	-0.82
β -Fe	-0.01	0.83	-0.82
γ -Fe	0.01	0.83	-0.84
δ -Fe	0.04	0.82	-0.86
ϵ -Fe	-0.01	0.85	-0.84
α -Ru	0.01	0.71	-0.72
β -Ru	0.01	0.71	-0.72
γ -Ru	-0.02	0.76	-0.74
δ -Ru	-0.01	0.79	-0.78
ϵ -Ru	0.02	0.76	-0.78
α -Os	0.20	0.46	-0.66
β -Os	0.20	0.44	-0.64
γ -Os	0.16	0.44	-0.6
δ -Os	0.16	0.55	-0.71
ϵ -Os	0.20	0.50	-0.70

248

249 In Table 5, the Azpy ligands carry positive charges while the chloride ligands carry negative charges.
 250 The charges on the metal atoms vary according to the nature of the atoms and the isomers. Here, the
 251 charges on Os are all positive regardless the isomer. However, in Fe and Ru complexes, the metallic
 252 charges depend on the *cis* or *trans* positions of the Cl atoms. While in the *cis* isomers (α -M, β -M and ϵ -

253 M) Fe displays negative charge, Ru charge regarding the same isomers are however positive.
254 Whereas in the *trans* isomers (γ -M and δ -M) both metals change their previous charge signs. The
255 charge values of the elements constituting these complexes indicate their role within the molecule.
256 The chloride ligands are electron donors and the Azpy ligand is an electron acceptor. The metal atom
257 is both a donor and an acceptor. Anyhow, the metal charges remain very low. This result agrees with
258 that found by Gottle et al. [29] in the theoretical study of metal-ligand interactions in isomers of the
259 $[\text{Ru}(\text{bpy})_2(\text{DMSO})_2]^{2+}$ complex by the NBO method. According to Bamba et al. [5], the ligand that has
260 the greatest natural charge in the molecule determines the affinity of the molecule to bind to DNA. In
261 the complexes studied, the Azpy has the largest charge. Thus, the isomers of each type of complex
262 were classified according to their ligand's charge. For the $\text{FeCl}_2(\text{Azpy})_2$ isomers, we have the following
263 order: QL (ϵ -Fe) > QL (α -Fe) > QL (γ -Fe) > QL (β -Fe) > QL (δ -Fe). As for the isomers of $\text{RuCl}_2(\text{Azpy})_2$
264 and $\text{OsCl}_2(\text{Azpy})_2$ complexes, we have respectively the following rankings: QL (δ -Ru) > QL (γ -Ru) > QL
265 (ϵ -Ru) > QL (α -Ru) > QL (β -Ru) and QL (δ -Os) > QL (ϵ -Os) > QL (α -Os) > QL (γ -Os) > QL (β -Os). These
266 results indicate that the ϵ -Cl isomers of the $\text{FeCl}_2(\text{Azpy})_2$ complexes and the δ -M isomers of the
267 $\text{RuCl}_2(\text{Azpy})_2$ and $\text{OsCl}_2(\text{Azpy})_2$ complexes are likely to bind easily to the DNA.

268 3.3- Anticancer effect of azopyridine complexes

269 Cancer is a family of illness related to many causes. Each cause can bring about a specific
270 type of cancer. El-Shahawy et al. defined cancer as a mutual transfer of electrons between
271 nucleic acid bases and an electron donor substrate or an electron acceptor, i.e. free radicals,
272 drugs and even certain foods such as grills and fries. According to them, the bases of the
273 nucleic acid generate carcinogenic cells by loss of electrons. In this process of electron
274 transfer, the bases of DNA can act as electron donors. This is the case for the metabolite of
275 Paracetamol in the liver that gives the N-acetyl-P-benzo-Quinone Imine (NAPQI) which has
276 higher electronic affinity to remove an electron from guanine in the nucleus of the liver cell in
277 the absence of glutathione [30]. As a result, the guanine base loses an electron producing a
278 guanine cation that can behave as a free radical. Positive cancer means that the nucleus
279 lacks an electron because of the mutual transfer of electrons. Therefore, it behaves
280 abnormally. This anomaly is related to the fact that electron loss can generate mutations of
281 certain genes that control cell replication. Therefore, this control system being faulty, the cell
282 begins to divide uncontrollably and becomes cancerous. In this work, the guanine cation will
283 be considered as the cancer cell. This type of cancer can be treated with drugs having a
284 spontaneous electron donor character under a certain condition to compensate the electron
285 deficiency. Organometallic complexes, particularly azopyridine complexes, may be potential
286 candidates for this role. The reasons are of various kinds, among which we have the
287 cytotoxicity of these complexes [31, 32, 8, 33]. Moreover, these complexes are
288 photosensitive [21]. Exposed to light, these complexes can emit electrons to fill the electronic
289 deficit of cancer cells. Therefore, it seems important to evaluate the effect of metals in these
290 complexes regarding the characteristics mentioned above.

291 3.3.1-Effect on cytotoxicity

292 Table 6 gathers the specific indices of reactivity such as the electronic chemical potential μ which
293 measures the tendency for electrons to escape from a molecule, the absolute chemical hardness η
294 which expresses the resistance of a system to change its number of electrons, electrophilia ω which
295 can be defined as its ability to bind strongly to a nucleophilic partner by electron transfer and
296 nucleophilicity N . Recently, Domingo et al. [19] showed that if a molecule is weakly electrophilic, then it
297 is systematically strongly nucleophilic and only true for simple molecules. For instance, captor-donor
298 ethylene (CD) and complex molecules bearing several functional groups can be both good
299 nucleophiles and good electrophiles [19]. Therefore, the nucleophile index cannot be defined as the
300 inverse of the electrophile. Domingo et al. [20] defined nucleophilicity as a negative value of the
301 ionization potential of the gas phase (intrinsic), IP, namely, $Nu = -IP$. So, high values of nucleophilicities
302 correspond to low values of ionization potentials and vice versa. Furthermore, Domingo et al. Used the
303 energies (HOMO) obtained by the Kohn-Sham method, $N = \epsilon_{\text{HOMO}}(\text{Nu}) - \epsilon_{\text{HOMO}}(\text{TCE})$ where

304 tetracyanoethylene (TCE) is the reference of its lowest energy of the HOMO among the series of
 305 molecules already explored in the context of organic polar reactions. This index has been successfully
 306 validated by available kinetic experimental data of molecules such like amines, diimines, anilines,
 307 alcohols, ethers, alkenes, and Π -nucleophiles.

308 Table 6: Specific Indices of Reactivity of Azopyridine Complexes in kcal.mol⁻¹

Isomer	μ	η	ω	N
α -Fe	-4.45	1.18	8.42	3.75
β -Fe	-4.40	1.12	8.61	3.86
γ -Fe	-4.46	1.18	8.41	3.73
δ -Fe	-4.43	1.16	8.50	3.79
ϵ -Fe	-4.45	1.10	9.01	3.83
α -Ru	-4.44	1.11	8.89	3.83
β -Ru	-4.37	1.15	8.32	3.85
γ -Ru	-4.38	1.01	9.48	3.99
δ -Ru	-4.33	0.90	10.43	4.15
ϵ -Ru	-4.38	1.02	9.41	3.98
α -Os	-4.44	1.13	8.70	3.81
β -Os	-4.35	1.20	7.89	3.83
γ -Os	-4.34	0.99	9.50	4.04
δ -Os	-4.25	0.82	10.96	4.31
ϵ -Os	-4.33	1.07	8.74	3.98
Cancer cell	-9.02	2.53	16.07	-2.18

309

310 The analysis of the values in this table indicates several trends. The values of the chemical potentials
 311 μ show that all these complexes are nucleophiles with chemical potentials μ which vary between -4,46
 312 and -4,25 relatively to the cancerous cells which will act as electron acceptors with a low chemical
 313 potential value of -9.02. β -Fe, δ -Ru and δ -Os isomers have the highest values respectively of -4.40; -
 314 4.33 and -4.25. Fortunately, these analyses are strengthened by the chemical hardness. Herein, the
 315 least resistant compound to the change of the number of electrons are β -Fe, δ -Ru and δ -Os. However,
 316 the most resistant for each type of isomer are assumed to be the γ -Fe, β -Ru and β -Os isomers.
 317 Besides, the cancer cells indicate the highest resistance with a chemical hardness value of 2.53
 318 kcal.mol⁻¹.

319 The nucleophile index makes it possible to establish a ranking according to the degree of nucleophilia.
 320 Thus, for the iron azopyridine complexes, there is the following classification: N (β -Fe) > N (ϵ -Fe) > N
 321 (δ -Fe) > N (α -Fe) > N (γ -Fe). The isomers of ruthenium and osmium have the following rankings: N (δ -
 322 Ru) > N (γ -Ru) > N (ϵ -Ru) > N (β -Ru) > N (α -Ru) and N (δ -Os) > N (γ -Os) > N (ϵ -Os) > N (β -Os) > N (α -Os).
 323 The negative value of the nucleophilia of cancer cells indicates that these cells can not engage
 324 electrons in interaction with other substrates. The electrophilia index indicates that they are the most
 325 electrophilic with a value of 16.07 kcal.mol⁻¹. From the foregoing, it can be deduced that the most
 326 active complexes are Os isomers. So, substitution of Ru with Os improves cytotoxicity.

327

328 **3.3.2-Effect on photosensitivity**

329 **3.3.2.1-Effect on the absorption of these compounds**

330 Absorption of each complex was performed using TDDFT calculations. These calculations make it
 331 possible to evaluate the sensitization capacity of these complexes. First, we proceed to an
 332 optimization followed by a calculation of frequency. The TDDFT calculation is performed on the
 333 minimum energy geometry. The level chosen for these calculations is the B3LYP / LanI2Z level.
 334 These azopyridine complexes are characterized by two types of electronic transitions $\pi \rightarrow \pi^*$ and t_{2g}
 335 $\rightarrow \pi^*$. The transitions $\pi \rightarrow \pi^*$ have high energy and have wavelengths less than 500 nm. These
 336 electronic transitions correspond to Ligand to Ligand Charge Transfer (LLCT). Whereas the $t_{2g} \rightarrow \pi^*$

337 transitions, they correspond to weak energy with their wavelengths beyond 500nm. They are assumed
 338 to represent the Metal to the Ligand Charge Transfer (MLCT). Table 7 lists the main transitions of
 339 each type, the energy (kcal.mol⁻¹), the maximum wavelength (nm), the oscillation force and the life
 340 time, the HOMO and LUMO orbitals of these complexes in their excited state. As for Table 8, it gives
 341 the percentage composition of the metal atom, the chlorine atoms and the Azpy ligand of the frontier
 342 orbitals involved in each transition selected in Table 7.

343 Table 7: Border orbitals with their percentage composition, energy (kcal.mol⁻¹), maximum
 344 wavelength (nm), oscillation force, life time of the main transitions of these complexes.

Isomers	HOMO(%)	LUMO(%)	ΔE (kcal.mol ⁻¹)	λ_{\max} (nm)	$f(L.M^{-1}.cm^{-1})$	τ (ns)	Main transition
α -Fe	Fe (42)	L (95)	2.76	449.96	0.062	48.79	HOMO ₅ → LUMO (77%)
			1.80	687.32	0.026	48.95	HOMO ₁ → LUMO ₊₁ (73%)
β -Fe	Fe (25)	L (91)	2.70	460.25	0.042	61.37	HOMO ₆ → LUMO (72%)
			1.67	743.51	0.019	75.61	HOMO ₂ → LUMO (76%)
γ -Fe	Fe (52)	L (99)	2.99	414.27	0.091	30.95	HOMO ₈ → LUMO (75%)
			1.60	773.62	0.028	28.27	HOMO ₁ → LUMO (81%)
δ -Fe	Fe (40)	L (100)	2.86	433.01	0.068	49.75	HOMO ₇ → LUMO (90%)
			1.53	812.62	0.023	41.33	HOMO ₁ → LUMO (92%)
ϵ -Fe	Fe (40)	L (97)	2.61	474.51	0.044	61.42	HOMO → LUMO (90%)
			1.49	833.87	0.016	76.71	HOMO ₁ → LUMO (87%)
α -Ru	Ru (46)	L (89)	2.92	424.41	0.070	48.32	HOMO ₅ → LUMO ₊₁ (41%)
			1.94	640.38	0.056	38.57	HOMO ₁ → LUMO ₊₁ (51%)
β -Ru	Ru (45)	L (86)	3.20	387.86	0.097	23.19	HOMO ₈ → LUMO (53%)
			1.85	671.17	0.038	23.25	HOMO ₁ → LUMO (84%)
γ -Ru	Ru (54)	L (93)	2.64	469.74	0.124	26.67	HOMO ₃ → LUMO (87%)
			2.04	607.07	0.096	26.68	HOMO ₂ → LUMO (79%)
δ -Ru	Ru (62)	L (98)	3.15	393.22	0.161	14.42	HOMO ₇ → LUMO (70%)
			1.51	821.66	0.059	14.40	HOMO ₅ → LUMO (77%)
ϵ -Ru	Ru (52)	L (90)	2.86	433.92	0.052	54.17	HOMO ₇ → LUMO (71%)
			1.71	726.85	0.045	54.28	HOMO ₂ → LUMO (59%)
α -Os	Os (50)	L (83)	3.35	370.25	0.092	22.32	HOMO ₄ → LUMO ₊₁ (65%)
			2.27	545.86	0.121	36.91	HOMO ₁ → LUMO ₊₁ (45%)
β -Os	Os (25)	L (91)	3.41	363.92	0.140	14.15	HOMO ₉ → LUMO (58%)
			2.24	552.30	0.115	14.18	HOMO ₂ → LUMO ₊₁ (77%)
γ -Os	Os (46)	L (84)	2.63	470.68	0.167	19.95	HOMO ₃ → LUMO (83%)
			2.22	557.80	0.221	21.11	HOMO ₂ → LUMO (48%)
δ -Os	Os (63)	L (91)	3.24	382.32	0.136	16.14	HOMO ₉ → LUMO (83%)
			1.65	753.36	0.064	16.17	HOMO ₁ → LUMO (74%)
ϵ -Os	Os (56)	L (83)	3.19	389.09	0.111	20.40	HOMO ₈ → LUMO (90%)
			2.09	592.36	0.094	20.53	HOMO ₂ → LUMO (52%)

345

346 TDDFT calculations indicate several electronic transitions of these complexes in the excited state. Two
 347 of these transitions for each complex have been selected in Table 7 according to the following criteria:
 348 the first transition is the most significant of the $\pi \rightarrow \pi^*$ transitions and the second is the most
 349 significant of the $t_{2g} \rightarrow \pi^*$ transitions. The most probable transitions of type $\pi \rightarrow \pi^*$ are those
 350 resulting from Os isomers. The most intense is that of the γ -Os isomer with a value of the oscillation
 351 force of 0.167 L.M⁻¹.cm⁻¹. This isomer absorbs at wavelength of 470.68nm. This transition is from the
 352 HOMO-3 to LUMO with a percentage of 83%. Actually, HOMO-3 Orbital of γ -Os is composed of 1%
 353 Os, 8% Chlorine and 91% Azpy in reference to Table 8. Whereas LUMO consists of 16% Os, 6%

354 Chlorine and 78% Azpy. Therefore, Os atom has very little influence on this transition. In general, the
 355 relative proportions of the metals in these $\pi \rightarrow \pi^*$ transitions are relatively small. This indicates that
 356 metals have a weak influence on these types of transitions. The other $\pi \rightarrow \pi^*$ transitions regarding
 357 Ru and Fe have relatively low intensities. When we observe the composition of the frontier orbitals
 358 involved in these transitions in Table 7, it is found that the HOMOs are mainly formed of orbitals from
 359 the chlorine atoms and the Azpy ligand and the LUMOs are mainly centered on the Azpy ligand. So,
 360 the electronic delocalization takes place from Cl atoms or Azpy to Azpy ligand. Therefore, it can be
 361 assumed that these transitions are of LLCT types.

362 As for the $t_{2g} \rightarrow \pi^*$ transitions, the most intense are also those resulting from Os isomers. However,
 363 the energies of these transitions are relatively high except for the δ -Os isomer which has an
 364 absorption band in the therapeutic window that comprise the absorption wavelength of 753.36 nm,
 365 with a life time of 16.17ns and an oscillation force of $0.064 \text{ L.M}^{-1}.\text{cm}^{-1}$ [37]. This transition is from
 366 HOMO-1 to LUMO with 74%. The HOMO-1 orbital of this isomer consists of 36% Os, 31% of Cl and
 367 33% of Azpy. Thus, the largest proportion comes from Os. Therefore, we can admit that osmium
 368 strongly influences this transition. The LUMO δ -Os orbital is made up of 9% Os, 3% Cl and 88% Azpy.
 369 So, this electronic transfer is directed mainly to the Azpy. Therefore, this transition is of the MLCT
 370 type.

371 Furthermore, for better use of light in Photo Dynamic Therapy PDT, the absorption band of the
 372 selected radiation should be far from the absorption bands of the human body's main tissue. In fact,
 373 the body components such as proteins, melanin and hemoglobin absorb in the UV and in the visible.
 374 For example, the absorption bands of hemoglobin are 280 nm, 410 nm, 540 nm, 580 nm and about
 375 600 nm [34]. Beyond 1000 nm, we have the absorption band of water thereby locating the therapeutic
 376 window between 600nm and 1000nm. Knowing that the absorption bands of $\pi \rightarrow \pi^*$ transitions are
 377 not in the therapeutic window; this transition series will thus be used only for treatments requiring a low
 378 penetration of light. In general, the $t_{2g} \rightarrow \pi^*$ transitions of these complexes can be involved in several
 379 therapeutic processes. For each type of complex, the isomers that provide the best characteristics are
 380 ϵ -Fe, δ -Ru and δ -Os. Besides, the most important contributions to these transitions generally come
 381 from metals. Here, Os provides the best contributions. So, osmium is the most suitable metal for
 382 ruthenium substitution in the context of improving therapeutic properties.
 383

384 Table 8: Contribution as a percentage of M = Fe, Ru, Os, Azpy and chlorine ligands in the OM_i orbitals
 385 (initial orbital) and OM_j (final orbital) of the main transitions of these complexes

Complexes	Transitions de type $\pi \rightarrow \pi^*$; $OM_i \rightarrow OM_i$						Transitions de type $t_{2g} \rightarrow \pi^*$; $OM_i \rightarrow OM_j$					
	Composition OM_i			Composition OM_i			Composition OM_i			Composition OM_j		
	M%	Cl%	Azpy%	M%	Cl%	Azpy%	M%	Cl%	Azpy%	M%	Cl%	Azpy%
α -Fe	22	56	22	5	2	93	3	88	9	14	2	84
β -Fe	37	43	20	9	2	89	25	66	10	29	2	90
γ -Fe	29	23	48	1	4	95	42	49	9	1	4	95
δ -Fe	37	35	28	0	5	95	51	41	8	0	4	96
ϵ -Fe	41	36	23	3	3	94	28	56	16	3	3	94
α -Ru	26	41	33	21	3	76	45	34	21	21	3	76
β -Ru	23	25	52	14	2	84	32	46	23	17	3	80
γ -Ru	1	82	17	7	4	89	74	3	23	7	4	89
δ -Ru	23	36	41	2	3	95	39	40	21	2	3	95
ϵ -Ru	22	27	51	10	1	89	26	48	26	10	1	89
α -Os	2	19	79	27	4	69	46	20	34	27	4	69
β -Os	37	20	43	9	1	90	36	31	33	23	4	74
γ -Os	1	8	91	16	6	78	69	26	29	16	6	78
δ -Os	12	41	47	9	3	88	36	31	33	9	3	88
ϵ -Os	2	0	98	17	2	81	29	36	34	17	1	82

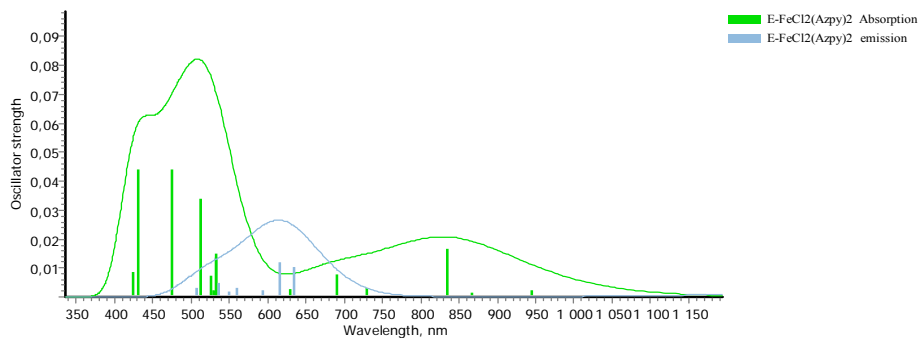
386 OM_i = initial orbital of transition OM_j = final orbital of transition

387 3.3.2.2-Effect on fluorescence characteristics

388 The isomers that provide the best absorption characteristics are selected here for fluorescence study.
 389 The emission and absorption spectra of these complexes (ϵ -Fe, δ -Ru and δ -Os) are represented in

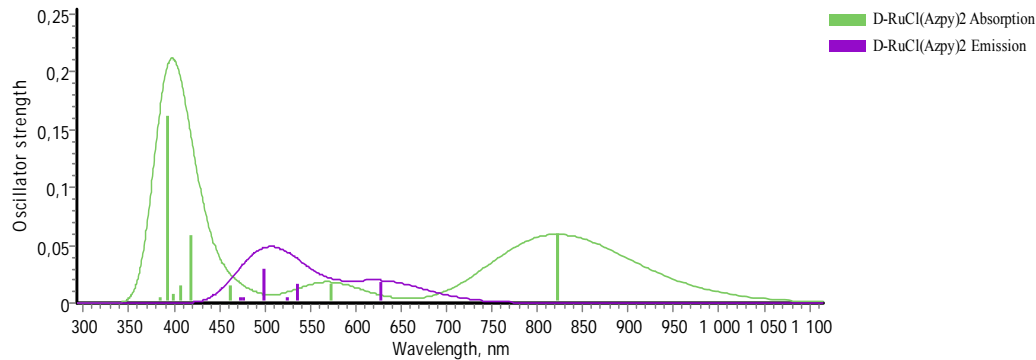
390 Figures 9, 10 and 11. These spectra indicate a bathochromic effect between the absorption and
391 emission spectra and a hypochromic effect due to charge and energy transfers. This bathochromic
392 effect that we notice is related to the energy losses that corresponds to the internal conversions and
393 the fluorescence phenomenon will take place for high wavelengths [35]. This shift of the absorption
394 and emission bands is crucial for better detection of the fluorescence signal. The charge and energy
395 transfer processes are favored by the presence of chlorine atoms. These photochemical processes
396 inhibit the fluorescence of azopyridine complexes.

397



398

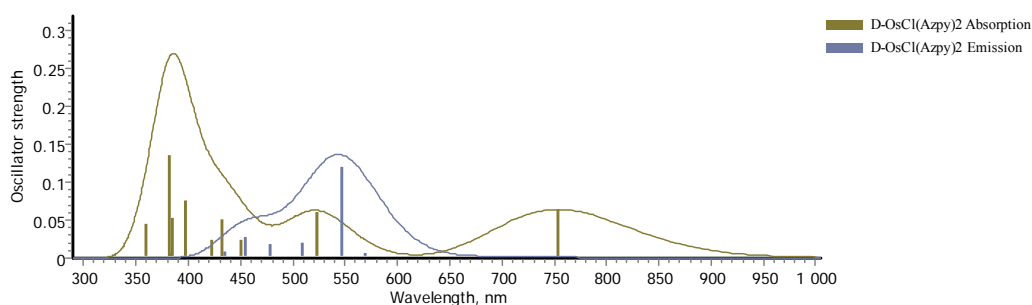
399 Figure 8: Emission and absorption spectrum of ϵ -Fe isomer in the gas phase at B3lyp / LAND2Z level.



400

401 Figure 9: Emission and absorption spectrum of δ -Ru isomer in the gas phase at B3lyp / LAND2Z level.

402



403

404 Figure 10: Absorption and emission spectrum of δ -Os isomer in gas phase at B3lyp / LAND2Z level.

405 To determine the capacity of ϵ -Fe, δ -Ru and δ -Os complexes to be engaged in a fluorescence
 406 process, we evaluated several parameters: First, the absorption wavelength λ_{Abs} that determines the
 407 absorption band of the molecule. Secondly, the Stokes shift (Ss) [36] which evaluates the ability for the
 408 molecule to distinguish between absorption and emission light. The detection of the fluorescence
 409 signal is a function of the value of the Stokes displacement. The larger it is, the better will be the
 410 detection of the fluorescence signal. Thirdly, the duration of the transition, also called the life time of
 411 the transition (τ) [37]. Fourthly, the energy of attachment of an exciton E_b [38] which is obtained by
 412 making the difference between the energy gap and the optical gap. An exciton is a pair comprising an
 413 electron and a hole linked by a Coulomb force (electrostatic) and located in the same region of space
 414 (orbital overlap). The exciton is formed when an electron passes from the HOMO band to the LUMO
 415 band and stays tied to the hole it left behind. It is a quasi-neutral particle that is treated as an
 416 hydrogenoid system and determines several optical and optoelectronic properties of the materials [39].
 417 Fifth, the extinction coefficient which is proportional to the intensity of the light emitted. In the absence
 418 of a phenomenon that can compete with the fluorescence process, the fluorescence intensity will so
 419 increase that the molar absorption coefficient will be higher for a given incident light intensity [37].

420 Table 9: Fluorescence spectrum parameters, wavelength absorption λ_{Abs} , Stokes shift (Ss), lifetime
 421 transition (τ), exciton.

Complexes	λ_{Abs} (nm)	Ss (nm)	τ (ns)	E_b (eV)	ϵ_{max}
ϵ -Fe	474.49	141.8	639.59	0.19	5200
δ -Ru	393.22	106.03	170.39	-0.69	10000
δ -Os	382.32	164.8	132.72	-1.1	16000

422 $Ss = \lambda_{max}(emission) - \lambda_{max}(absorption)$ $E_b = \Delta E_{L-H} - E_{flu}$ $E_{flu} = \frac{1240}{\lambda_{max}(em)}$

423 Table 9 indicates that ϵ -Fe has the absorption band having the lowest energy with 474.49 nm as a
 424 value of λ_{Abs} . However, δ -Os provides the best fluorescence characteristics. This isomer best
 425 distinguishes the light emitted and the light absorbed. This is observed by the value of its stokes
 426 displacement which is 164.8 nm. It has the shortest life time estimated at 132.72 ns. This enhances
 427 fluorescence activity and minimizes other forms of energy conversion [39]. It has the lowest
 428 attachment energy of excitons. This improves its ability to emit photons and this is confirmed by its
 429 molar extinction coefficient which is of the order of 16000. All these metal complexes have a
 430 conventional life time comprised between 10^{-10} to 10^{-7} s [36]. Besides, ϵ -Fe isomer has the longest life
 431 time of 639.59 ns. This indicates that in this complex we have a facility of transfer of energy and
 432 electrons [39]. Moreover, the analysis of the transitions giving rise to this fluorescence has been
 433 characterized by the Einstein parameters. These parameters are recorded in Table 10. The
 434 spontaneous emission probability coefficient and the spontaneous absorption probability coefficient.
 435 Two parameters are added to the wavelength at which these transitions occur, the oscillation force
 436 and the dipole moment of these transitions.

437 Table 10: Fluorescence spectrum parameters, Einstein probability coefficients (A_{if} and B_{if}), dipole
 438 moment transition (D_{if}) and oscillation force (F_{if}) of complex Azpy at B3LYP / LANLD2Z level

Isomères	λ_i (nm)	$A_{ij} \times 10^{-13} s^{-1}$	$B_{ij} \times 10^{-8} sg^{-1}$	D_{ij}	f_{ij}
ϵ -Fe	833,95	1,563	9,691	0,668	0,0163
δ -Ru	821,66	5,869	1,84	1,27	0,059
δ -Os	753,35	7,534	18,281	1,261	0,0641

439

440 The parameters in Table 10 confirm the performance of δ -Os as It has the highest values.
 441 This isomer possesses the most probable emission and absorption with spontaneous
 442 emission probability coefficients A_{if} and spontaneous absorption coefficients B_{ij} respectively
 443 $7.534 \times 10^{-13} s^{-1}$ and $18.281 sg^{-1}$. The dipole moments of transition are arranged in the order D_{ij}
 444 (δ -Ru) > D_{ij} (δ -Os) > D_{ij} (ϵ -Fe). As for the oscillating forces, we have the following order: f_{ij} (δ -
 445 Os) > f_{ij} (δ -Ru) > f_{ij} (δ -Os). The results in Tables 9 and 10 indicate that the best fluorophore is the δ -Os
 446 isomer [40]. Thus, the substitution of ruthenium by Osmium in the azopyridine complexes increases
 447 the fluorescence.

448 4. CONCLUSIONS

449 The theoretical exploration of the azopyridine metal complexes such as the α -, β -, γ -, δ -, ϵ -MCl₂
 450 (Azpy)₂ isomers with M = Fe, Os and Ru was carried out in this work with the DFT and TDDFT
 451 methods. It showed that the presence of metal within these complexes played a crucial role. The
 452 structural analysis carried out on these complexes revealed that all the bonds of MX (with X = Cl, N₂,
 453 N_{py}) underwent an increasing elongation from the iron to the osmium passing through ruthenium.
 454 Furthermore, Reactivity, stability, and solubility in organic solvents also evolve following the same
 455 trend. Whereas the evaluation of the transitions of the excited states indicates that the second
 456 absorption bands of all the isomers were in the therapeutic window except for osmium isomers of
 457 which only δ -Os fulfills this condition. This analysis indicates that these azopyridine complexes could
 458 be used in photodynamic therapy. Above all, it can be assumed that the activity of azopyridine Ru
 459 complexes can be increased by replacing Ru by Os, namely by using δ -OsCl₂(Azpy)₂.

460

461 RÉFÉRENCES

462

- [1] L. Torre, F. Bray, R. Siegel, J. Ferlay, J. Lortet-Tieulent et A. Jemal, «Global Cancer Statistics 2012.CA:», *A Cancer Journal for Clinicians*, 2015; vol. 65, pp. 87-108.
- [2] C. Sun, Y.Li, P. Song et F.Ma, «An Experimental and Theoretical Investigation of the Electronic Structures and Photoelectrical Properties of Ethyl Red and Carminic Acid for DSSC Application», *Materiels*. 2016; vol. 9, p. 813.
- [3] B. A. Sava G, «NAMI-A., Influence of chemical stability on the activity of the antimetastasis ruthenium compound,» *Eur. J. Cancer*. 2002; vol. 38, p. 427–435.
- [4] A. Bergamo, «Modulation of the metastatic progression of breast cancer with an organometallic ruthenium compound.,» *Int. J. Oncol*. 2008; vol. 33, p. 1281–1289.
- [5] K. Bamba, O. W. Patrice, N. K. Nobel et N. Ziao, «SARs investigation of α -, β -, γ -, δ -, ϵ -

- RuCl₂(Azpy)₂ complexes as Antitumor drugs.,» *Computational Chemistry*. 2015; vol. 4, pp. 1-10.
- [6] R. A. Krause et K. Krause, Chemistry of bipyridyl-like ligands. Isomeric complexes of ruthenium(II) with 2-(phenylazo)pyridine, *Inorg. Chem.* 1980; vol. 19, pp. 2600-2603.
- [7] A. H. Velders, H. Kooijman, A. L. Spek, J. G. Haasnoot, D. de Vos et Reedijk, *J. Inorg. Chem.* 2000; vol. 39, pp. 2966-2967.
- [8] G. A. Hotze, E. S. Casper, D. Vos, H. Kooijma, L. A. Spek, A. Flamigni, M. Bacac, G. Sava, G. J. Haasnoot et J. Reedijk, «structure-dependent in vitro cytotoxicity of the isomeric complexes [Ru(L)2Cl2] (L=o-tolylazopyridine and 4- methyl-2-phenylphenylazopyridine) in comparison to [Ru(azpy)2Cl2],» *J. Biol. Inorg. Chem.* 2004; vol. 9, p. 354–364.
- [9] N. K. Nobel, W. P. Ouattara, K. Bamba et N. Ziao, «Theoretical calculation of influence of halogen atoms (F, Cl, Br, I) on arylazopyridine (Azpy) ruthenium complexes behaving as photo sensitizers byDFT method,,» *International Journal of Advanced Chemistry*. 2018; vol. 6, pp. 67-73.
- [10] M. Frisch, G. Trucks, H. Schlegel, G. Scuseria, M. Robb, J. Cheeseman, G. Scalmani, V. Barone, B. Mennucci, G. Petersson, H. Nakatsuji, M. Caricato et X. Li, «M. Hada, M. Ehara, K. Toyota, R. Fukuda, J. Hasegawa, H.P. Hratchian, A.F. Izmaylov, J. Bloino, G. Zheng, J.L. Sonnenberg, M. Hada, M., M. Ishida, T. Nakajima, Y. Honda, O. Kitao, H. Nakai, T. Vreven, J.A. Montgomery, Jr., J.E. Peralta,,» *F. Ogliaro, M. Bearpark, J.J. Heyd, E. Brothers, K.N. Kudin, V.N. Staroverov, T. Keith, R. Kobayashi, J. Fox, ?Gaussian 09 (Gaussian, Inc., Pittsburgh, PA,),*, p. 1995–2011.
- [11] A. D. Becke, A new mixing of Hartree–Fock and local density-functional theories, *J. Chem. Phys.* 1993; vol. 98, p. 1372.
- [12] A. Görling, Density-functional theory for excited states, *Phys. Rev. A*, 1996; vol. 54, p. 3912.,
- [13] J. Foresman et Æ. Frisch, «Exploring Chemistry with Electronic Structure Methods, second ed.,» *Gaussian Inc., Pittsburgh, PA,* , 1996.
- [14] P. Hohenberg et W. Kohn, Inhomogeneous Electron Gas, *Phys. Rev. B*, 1964; vol. 136, p. 864.
- [15] P. J. Hay et W. R. Wadt, Ab initio effective core potentials for molecular calculations. Potentials for the transition metal atoms Sc to Hg, *J. Chem. Phys.* 1985; vol. 82, p. 270.
- [16] W. R. Wadt et P. J. Hay, Ab initio effective core potentials for molecular calculations. Potentials for main group elements Na to Bi, *J. Chem. Phys.* 1985; vol. 82, p. 284.
- [17] C. Adamo, E. Rebolini et A. Savin, *l'actualité chimique* , pp. n° 382-383, février-mars 2014.
- [18] A. Juris, V. Balzani, F. Barigelletti, S. Campagna, P. Belser et A. Zelewsky, Ru(II) polypyridine complexes: photophysics, photochemistry, eletrochemistry, and chemiluminescence, *Coord. Chem. Rev.* 1988; vol. 84, p. 85.,
- [19] L. R. Domingo, M. Aurell, P. Perez et R. Contreras, Quantitative characterization of the global electrophilicity power of common diene/dienophile pairs in Diels–Alder reactions, *Tetrahedron*, 2002; vol. 58, p. 4417.
- [20] L. R. Domingo, E. Chamorro, P. Perez, P. Jaramillo, L. R. Doming, E. Chamorro et P. Perez,

Understanding the Reactivity of Captodative Ethylenes in Polar Cycloaddition Reactions. A Theoretical Study, *J. Org. Chem.* 2008; 73, 4615.

- [21] N. K. Nobel, K. Bamba, O. W. Patrice et N. Ziao, «NBO Population Analysis and Electronic Calculation of Four Azopyridine Ruthenium Complexes by DFT Method.,» *Computational Chemistry*, 2017; vol. 5, pp. 51-64.
- [22] P. Pavita, j. prashanth, G. Ramu, G. Ramesh, K. M. Reddy et B. V., Synthesis, structural, spectroscopic, anti-cancer and molecular docking studies on novel 2-[(Anthracene-9-ylmethylene)amino]-2-methylpropane-1,3-diol using XRD, FTIR, NMR, UV-Vis spectra and DFT, *journal of molecular structure*. 2017; vol. 1147, pp. 406-426.
- [23] D. F. Shriver et P. Atkins, « *Inorganic Chemistry*, » 3rd Edition. New York: Oxford University Press., 1999.
- [24] D. Lerner, S. Balaceanu, C. Weinberg et J. L. Patron, «Computational Study of the Molecular Complexes between 5-HTP with ATP and DHEA. Potential New Drug Resulting from This Complexation.,» *Computational Chemistry*, ,, vol. 3, pp. 18-22., 2015.
- [25] K. Fukui, T. Yonezawa et H. Shingu, «A Molecular Orbital Theory of Reactivity in Aromatic Hydrocarbons.,» *J. Chem. Phys.* 1952; vol. 20, p. 722.
- [26] L. Salem, «Intermolecular orbital theory of the interaction between conjugated systems. I. General theory.,» *J. Am. Chem. Soc.*, vol. 9, p. 543., 1968.
- [27] G. Klopman, «Chemical reactivity and the concept of charge- and frontiercontrolled reactions, ,,» *J. Am. Chem. Soc.* 1968; vol. 90, p. 223.
- [28] R. Daniel, M. Rubio, M. Manuela et S. Luis, Ab initio determination of the ionization potentials of DNA and RNA nucleobases, *the journal of chemical physics*, 2006; vol. 125, p. 084302.
- [29] A. GÖTTLE, «mémoire de thèse,» université de TOULOUSE, 2013.
- [30] A. El-Shahawy, «DFT Cancer Energy Barrier and Spectral Studies of Aspirin, Paracetamol and Some Analogues.,» *Computational Chemistry*, 2014; vol. 2, pp. 6-17.
- [31] E. Wong et C. M. Giandomenico, «Current Status of Platinum-Based Antitumor Drugs.,» *Chem. Rev.* 1999; vol. 99, pp. 2451-2466.
- [32] A. Velders, H. Kooijman, A. Spek, J. Haasnoot, D. De Vos et J. Reedijk, «Strong Differences in the in Vitro Cytotoxicity of Three Isomeric Dichlorobis (2-Phenylazopyridine) Ruthenium(II) Complexes.,» *Inorganic Chemistry*, 2000; vol. 39, pp. 2966- 2967.
- [33] A. Hotze, A. Velders, F. Ugozzoli, M. Biagini-Cingi, A. Manotti-Lanfredi, J. Haasnoot et J. Reedijk, «Synthesis, Characterization, and Crystal Structure of α -[Ru(azpy)₂(NO₃)₂] (azpy =2-(Phenylazo) Pyridine) and the Products of Its Reactions with Guanine Derivatives.,» *Inorganic Chemistry*, 2000; vol. 39, pp. 3838-3844.
- [34] I. Rodica-Mariana, Photodynamic therapy (PDT): a photochemical concept with medical applications, *Revue Roumaine de Chimie*, 2007; vol. 52, p. 1093–1102.

- [35] T. CARON, «l'ecole nationale superieure de chimie de montpellier,,» *mémoire de thèse,,* p. 16, 2010.
- [36] A. Hlel, A. Mabrouk, M. Chemek, I. Ben Khalifa et K. Alimi, *Computational Condensed Matter*, 2015; vol. 3, pp. 30-40.
- [37] V. Lukes, A. Aquino et H. Lischka, Theoretical Study of Vibrational and Optical Spectra of Methylene-Bridged Oligofluorenes, *J. Phys. Chem. A*, 2005; vol. 109, pp. 10232-10238.
- [38] P. Françoise, *mémoire de thèse, Université de Montréal*, p. 28., 2013.
- [39] M. Hachi, S. E. Khattabi¹, A. Fitri¹, A. Benjelloun, M. Benzakour, M. Mcharfi, M. Hamidi et M. Bouachrine⁴, *J. Mater. Environ. Sci.*, 2018; vol. 9 , pp. 1200-121.
- [40] Y. Zhang, L. Zhang, R. Wang et X. Pan, «Theoretical Study on the Electronic Structure and Optical Properties of Carbazole- π -Dimesitylborane as Bipolar Fluorophores for Nondoped Blue OLEDs.,» *J. Mol. Graph. Model.* 2012; vol. 34, p. 46–56.

463

464